

ORGANISATION EUROPÉENNE POUR LA RECHERCHE NUCLÉAIRE
CERN EUROPEAN ORGANIZATION FOR NUCLEAR RESEARCH

A NEW POSITION-SENSITIVE DETECTOR
FOR THERMAL AND EPITHERMAL NEUTRONS

A.P. Jeavons, N.L. Ford, B. Lindberg and R. Sachot

GENEVA
1977

© Copyright CERN, Genève, 1977

Propriété littéraire et scientifique réservée pour tous les pays du monde. Ce document ne peut être reproduit ou traduit en tout ou en partie sans l'autorisation écrite du Directeur général du CERN, titulaire du droit d'auteur. Dans les cas appropriés, et s'il s'agit d'utiliser le document à des fins non commerciales, cette autorisation sera volontiers accordée.

Le CERN ne revendique pas la propriété des inventions brevetables et dessins ou modèles susceptibles de dépôt qui pourraient être décrits dans le présent document; ceux-ci peuvent être librement utilisés par les instituts de recherche, les industriels et autres intéressés. Cependant, le CERN se réserve le droit de s'opposer à toute revendication qu'un usager pourrait faire de la propriété scientifique ou industrielle de toute invention et tout dessin ou modèle décrits dans le présent document.

Literary and scientific copyrights reserved in all countries of the world. This report, or any part of it, may not be reprinted or translated without written permission of the copyright holder, the Director-General of CERN. However, permission will be freely granted for appropriate non-commercial use.

If any patentable invention or registrable design is described in the report, CERN makes no claim to property rights in it but offers it for the free use of research institutions, manufacturers and others. CERN, however, may oppose any attempt by a user to claim any proprietary or patent rights in such inventions or designs as may be described in the present document.

ABSTRACT

A new two-dimensional position-sensitive neutron detector is described. It is based on (n,γ) neutron resonance capture in a foil with subsequent detection of internal conversion electrons with a high-density proportional chamber. Large-area detectors with a 1 mm spatial resolution are feasible. A detection efficiency of 50% is possible for thermal neutrons using gadolinium-157 foil and for epithermal neutrons using hafnium-177.

CONTENTS

	<u>Page</u>
1. INTRODUCTION	1
2. THE BASIC DETECTOR	1
2.1 The foil converter	2
2.2 The high-density proportional chamber	4
3. EXPERIMENTAL RESULTS	5
3.1 Chamber construction	5
3.2 Detection efficiency	6
3.3 Spatial resolution	6
3.4 Background	6
4. CONCLUSION	7
REFERENCES	9

1. INTRODUCTION

Gas proportional chambers are currently in use as position-sensitive detectors for neutron small-angle scattering^{1,2)}. For neutron crystallography a detector must maintain its spatial resolution out to large angles of neutron incidence. Conventional gas detectors cannot do this because of the thickness of the conversion space. Either a very thin, high-pressure detector, or a pressurized spherical drift chamber³⁾ is needed, both of which pose difficult technological problems. Scintillation screens are an alternative approach⁴⁾, but they have not yet achieved reliable operation.

A new technique, which uses a thin foil for neutron conversion and a high-density proportional chamber⁵⁾ for detection, is described here. The separation of the converter and detector functions permits independent optimization. For the foil a material with a large neutron absorption cross-section is required. Boron and lithium (n,α) are well known, but they provide only a low detection efficiency⁶⁾. A material with a much higher thermal neutron cross-section, due to an (n,γ) resonance, is gadolinium. Electrons are efficiently produced by internal conversion. For epithermal neutrons, hafnium, with similar properties to gadolinium except for the higher energy resonance, may be used.

2. THE BASIC DETECTOR

Figure 1 illustrates the basic detector. There are three parts: the foil converter, which produces electrons; the high-density drift space, which traps each electron and restricts its range thus providing good spatial resolution; and the proportional chamber, which receives the ionization from the drift space and records the (x,y) coordinates.

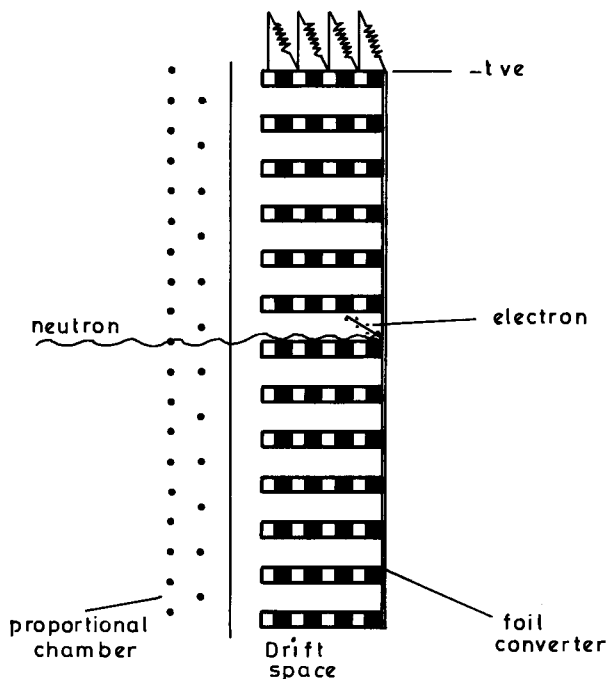


Fig. 1 The basic detector

2.1 The foil converter

Gadolinium-157 has the very large thermal neutron absorption cross-section of 250,000 b owing to an (n,γ) resonance at 0.031 eV⁷⁾. In addition, the first excited state of the nucleus at 79.3 keV has a total transition probability to the ground state of 0.75⁸⁾ combined with an internal conversion probability of 0.85⁹⁾. The transition from the second excited level at 261 keV to the first also provides electrons. Depending on whether the internal conversion is on the K, L, M, or N shells, an electron will be emitted with an energy in the range 29-182 keV¹⁰⁾. From these properties it follows that a foil, thick enough to absorb neutrons efficiently, has a high probability of producing electrons and will still be thin enough to allow the electrons to escape from the foil and be detected.

The possibility of using gadolinium for detecting thermal neutrons was noted many years ago¹¹⁾. Combined with surface barrier detectors, a practical system has been demonstrated^{12,13)}.

The theoretical analysis developed previously^{5,14)} for photon detection may be applied here to calculate the detection efficiency as a function of foil thickness and for any particular neutron energy.

Consider a neutron capture occurring at a depth x below the surface of a foil of thickness t . The electron produced will have two escape possibilities: the back-scattered and transmission directions. If these two cases are considered independently, then they correspond to electron transmission through foils of thickness x and $(t - x)$, say probabilities P_1 and P_2 . Then the net probability for the foil is

$$P_1 | P_2 = P_1 + P_2 - P_1 P_2 .$$

The total efficiency ϵ , is found by including the neutron absorption probability and integrating over x :

$$\epsilon = \frac{\int_0^t \exp\left(-\frac{x}{\tau}\right) \left(P_1 + P_2 - P_1 P_2\right) dx}{\int_0^{\infty} \exp\left(-\frac{x}{\tau}\right) dx} ,$$

where τ is the absorption attenuation length, i.e.

$$\epsilon = \frac{1}{\tau} \int_0^t \exp\left(-\frac{x}{\tau}\right) \left(P_1 + P_2 - P_1 P_2\right) dx . \quad (1)$$

P_1 and P_2 are known:

$$P_1 = \exp A \left(1 - \frac{x}{R}\right)^P \exp \left[-A \left(1 - \frac{x}{R}\right)^{-1} \right]$$

$$P_2 = \exp A \left(1 - \frac{t-x}{R}\right)^P \exp \left[-A \left(1 - \frac{t-x}{R}\right)^{-1} \right] ,$$

where A and P are constants, and R , the electron residual range, is a function of electron energy.

Equation (1) has been evaluated numerically for the six contributions K, L, M and N for 79.3 and 182 keV of gadolinium. The results are shown graphically in Fig. 2 for ¹⁵⁷Gd and ^{nat}Gd and tabulated in Table 1. Moderately high efficiencies are evident. One important

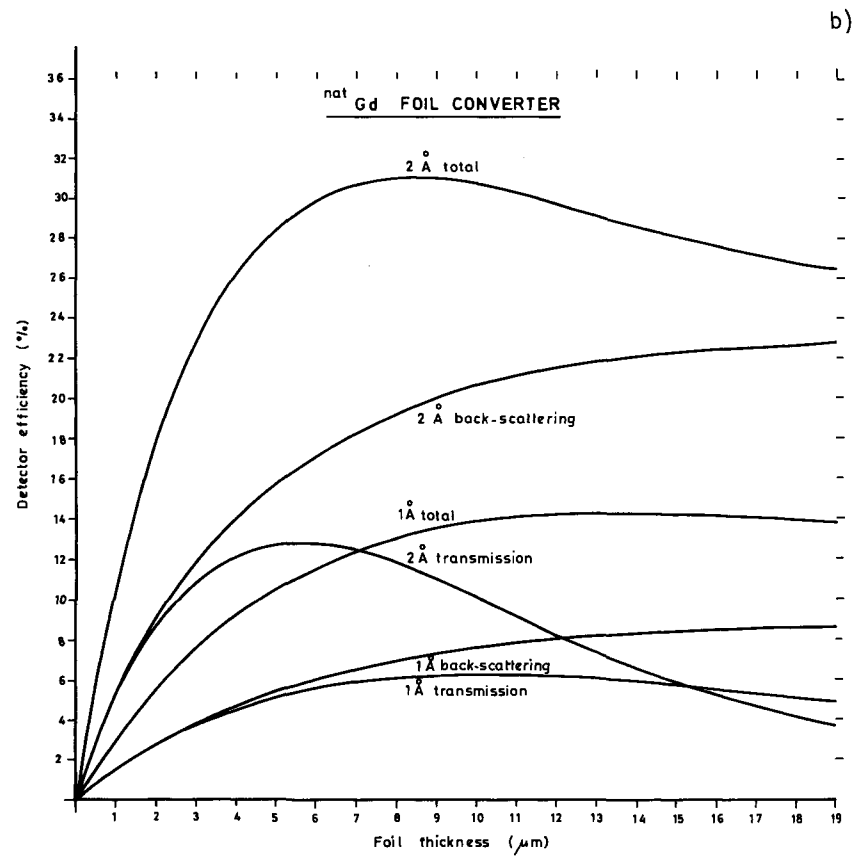
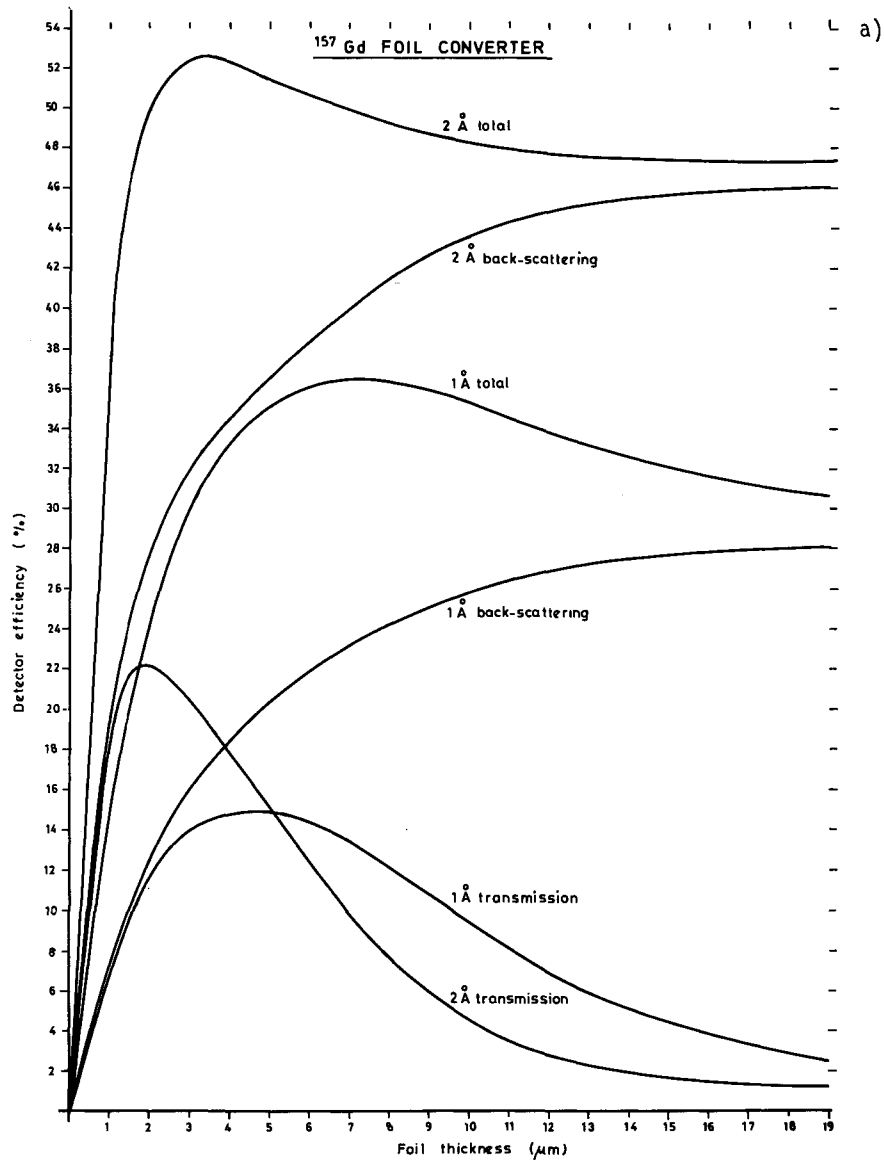


Fig. 2 a) Theoretical detection efficiencies for gadolinium-157
 b) Theoretical detection efficiencies for natural gadolinium

Table 1

Detection efficiencies for gadolinium foil converters. The total is not the sum of back-scattering and transmission, as each figure is for the optimum foil thickness. Note that the back-scattering dominates.

Material	Neutron wavelength Å	Efficiencies (%)		
		Maximum back-scattering	Maximum transmission	Maximum total
¹⁵⁷ Gd	4	53	25	58
	2	47	22	53
	1	29	15	37
	0.7	9	6.5	14
nat Gd	4	31	16	39
	2	24	13	31
	1	9	6.5	14
	0.7	2	2	4

point emerges that has not been widely appreciated. It is the back-scattered contribution that dominates, being about twice as large as the maximum transmission value. This fact stems from the multiple scattering of electrons in matter: the direction of the incoming neutron is of no significance. The electrons will simply escape preferentially to the closest surface, which for the majority will be the front surface, due to the exponential absorption. The highest efficiencies are obtained by collecting from both sides of a foil of optimum thickness, but in general the back-scattered efficiency of a thick sheet is nearly as good.

Other resonances may be used to obtain similar detection efficiencies at shorter neutron wavelengths. The choice is restricted to stable parent and product nuclides that also show the high internal conversion probability. Table 2 lists some possibilities. Hafnium-177 is particularly interesting for epithermal neutrons. Unfortunately, ¹⁴⁹Sm and ¹¹³Cd with strong resonances in a useful wavelength region have a much higher first excited-state energy than gadolinium and do not show much internal conversion.

2.2 The high-density proportional chamber

The high-density drift space consists of a sandwich of alternately conducting and insulating sheets, perforated with a regular hole pattern. The conducting sheets are connected via a resistor chain. Applying a voltage to the chain produces a drift field in the holes. Then any ionization created by an electron from the foil trapped in the hole will be extracted and passed to the proportional chamber, where it will create an avalanche. For the original application to gamma-ray detection, the drift space served two functions: photon to electron conversion and electron range limitation. For this application, only the range-limiting property is required. In fact the photon sensitivity of the drift space is a disadvantage.

Table 2

Resonances with a stable parent and product nuclide. K-shell X-rays following neutron capture indicate the degree of internal conversion.

Nuclide	Resonance energy (eV)	Cross-section (b)	K-shell X-rays (% n capture)	Comment
^{155}Gd	0.0268	58000	25	^{157}Gd better
^{157}Gd	0.0314	230000	25	Useful
^{149}Sm	0.0976	132000	3.7	Low efficiency
^{113}Cd	0.1776	62000	1.1	Low efficiency
^{180}Ta	0.433	12000	81?	Very low isotropic abundance Expensive
^{167}Er	0.460	10100	32	Resonance not very strong
^{149}Sm	0.872	20600	3.7	Low efficiency
^{177}Hf	1.098	34600	41	Useful
^{177}Hf	2.38	75000	41	Useful

Construction of the space must minimize photon and neutron interactions by using low-density materials.

The proportional chamber serves purely as a read-out device. Construction may follow traditional techniques¹⁵⁾. Details of electronic read-out may also be found elsewhere^{16,17)}.

3. EXPERIMENTAL RESULTS

To test the ideas described in the previous section, a small chamber with an active area of 4×4 cm has been constructed and tested in a neutron beam at the Institut Laue-Langevin, Grenoble, France (ILL).

3.1 Chamber construction

Proportional chamber construction follows normal methods. Wires were of gold-plated tungsten: anode wires 20 μm diameter, 1.5 mm spacing; and cathode 100 μm , 1 mm spacing. The anode-cathode gap was 3 mm. Pure isobutane was used as the chamber gas. The operating voltage on the anode plane was 4 kV. Read-out was by the centre-of-gravity technique¹⁸⁾ using CAMAC analogue-to-digital converters and an LSI11 computer displaying on a Tektronix 4010 terminal.

The drift space was made of 0.1 mm thick sheets of aluminium and "VETRONITE" epoxy-resin drilled with holes of 0.85 mm diameter on a hexagonal pattern of pitch 1 mm. The total thickness of the sheets was 3 mm. A 25 μm thick sheet of $^{\text{nat}}\text{Gd}$ was used for the neutron converter.

3.2 Detection efficiency

The detection efficiency was measured on the D12 system in the neutron guide hall of the ILL. The detector was aligned in the back-scattering configuration onto a sodium chloride reflection, previously measured with a ^3He counter to be 200 counts sec^{-1} . A count rate of 44 sec^{-1} was recorded, i.e. a detection efficiency of 22%. This is in good agreement with the theoretical figure of 21.5% for 1.8 \AA neutrons.

3.3 Spatial resolution

Three holes were drilled in a line in a piece of cadmium. Each hole was 1 mm in diameter; the first two holes were spaced at 3 mm and the third at 5 mm. This sheet was placed in the neutron beam and in front of the chamber. The chamber response is shown in Fig. 3. Figure 3a shows the two-dimensional distribution. The small spots correspond to the individual holes of the drift space. Each group of these small spots comes from a hole in the cadmium. Figure 3b is a cross-section through the line of holes with intensity as the vertical scale. There are four bins per mm. Both the 5 mm and 3 mm spacings are completely resolved. The over-all spatial resolution is the envelope of each group of spots -- clearly a FWHM of about 1 mm, as expected. The resolution was checked with the beam angled at 30° to the detector. No degradation was observed.

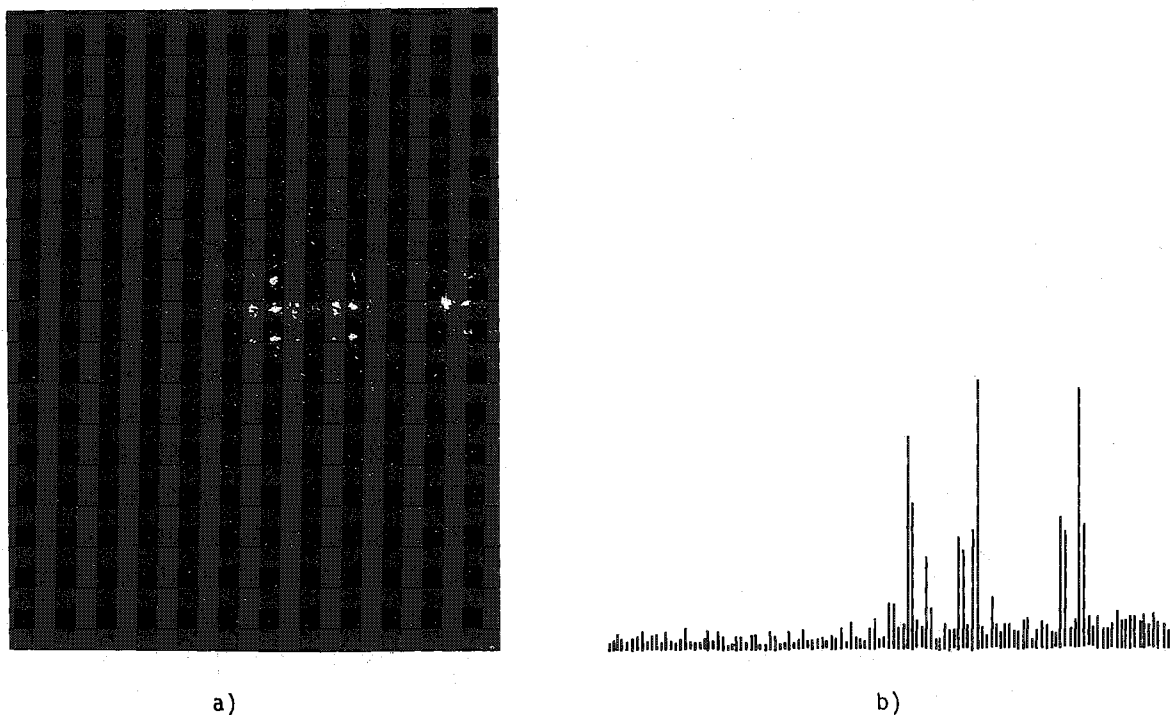


Fig. 3 a) The neutron image of three holes in a cadmium sheet. Each of the small spots is a hole in the drift space, spaced at 1 mm.
b) A cross-section through the above image, showing neutron intensity. There are four bins per mm.

3.4 Background

Like the neutron signal, photons will produce electrons in the chamber -- by photoelectric absorption and Compton scattering. This background may be minimized by making the chamber as transparent as possible to gamma-rays. In addition, the chamber may be screened from photons with an energy < 200 keV with a few mm of lead. Higher energy photons may be filtered out electronically by the different type of event that they produce in the chamber. High-energy electrons will not be trapped in the holes of the drift space but will traverse the whole chamber leaving tracks of extended ionization. This causes avalanches on more than one anode wire and pulses of much slower rise-time. An example of the rise-time difference is shown in Fig. 4. The neutron signal produces a sharp peak at short rise-time, whilst the gamma-ray background is a flat distribution. This kind of discrimination is obviously analogous to that used in solid-state neutron detectors.

By the above methods, a background level of about $1 \text{ count sec}^{-1} \text{ cm}^{-2}$ was achieved in the detector in the ILL guide-hall environment. Further work should reduce this level.

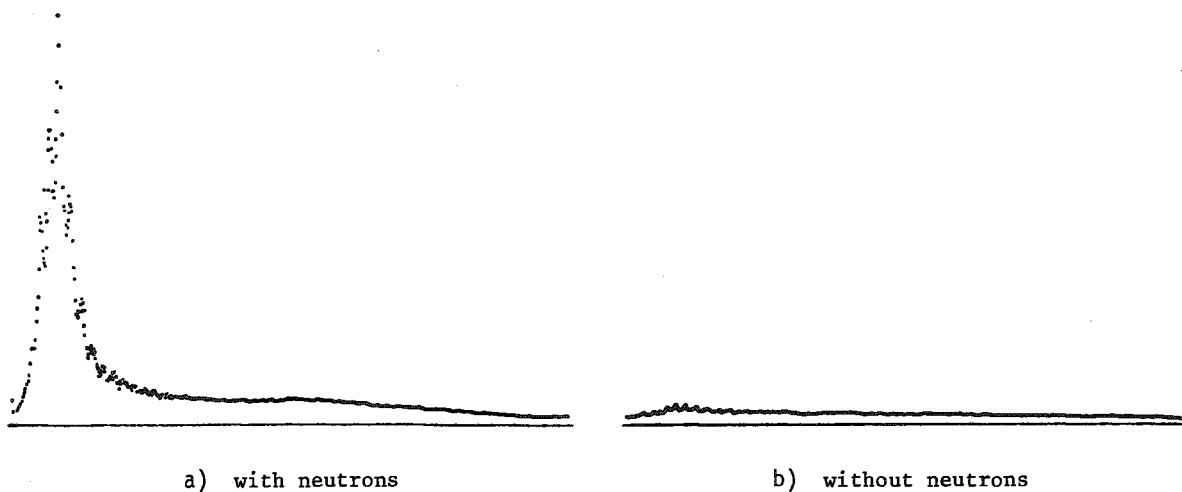


Fig. 4 The pulse rise-time spectrum from the detector. Full scale 100 nsec.

4. CONCLUSION

The detector described here promises a number of important advantages for neutron detection:

- i) Two-dimensional spatial resolution of 1 mm or better, independent of the neutron incident angle.
- ii) A detection efficiency of 50% for thermal and epithermal neutrons.
- iii) Adequate background rates: $< 1 \text{ count sec}^{-1} \text{ cm}^{-2}$ in a guide-hall environment.
- iv) Large area detectors -- say $1 \times 1 \text{ m}$ -- are feasible.

v) Free flow gas at atmospheric pressure in the chamber implies no outgassing, purity, or pressure problems.

vi) Digital electronic read-out is stable and free from drift.

The experimental and theoretical results obtained to date confirm these points.

Acknowledgements

We wish to thank J. Jacobe and his colleagues for assistance with the tests at the ILL. In particular, we thank Dr. H. Bartunik for many discussions, and for his encouragement and support over a long period.

REFERENCES

- 1) J. Jacobe, ILL Internal Scientific Report 75M42 (1975), p. 20-57.
- 2) J. Alberi, J. Fischer, V. Radeka, L.C. Rogers and B. Schoenborn, IEEE Trans. Nuclear Sci. NS-22, 255 (1975).
- 3) G. Charpak, Z. Hajduk, A.P. Jeavons, R. Kahn and R.J. Stubbs, Nuclear Instrum. Methods 122, 307 (1974).
- 4) D. Gilmore, ILL Internal Scientific Report 75M42 (1975), p. 88-102.
- 5) A.P. Jeavons, G. Charpak and R.J. Stubbs, Nuclear Instrum. Methods 124, 491 (1975).
- 6) B.H. Meardon and D.C. Salter, RHEL/R 262 (1972).
- 7) S.F. Mughabghab and D.I. Garber (eds.), Neutron cross-sections, BNL 325 (1973), vol. 1.
- 8) J.K. Tuli, Nuclear Data Sheets 12, No 2, 245-304 (1974).
- 9) P.S. Hager and E.C. Seltzer, Nuclear Data A4, Nos 1 and 2 (1968).
- 10) L.V. Groshev, A.M. Demidov, V.A. Ivanov, V.N. Lutsenko and V.I. Pelekhov, Izv. Akad. Nauk SSSR, Ser. Fiz. 26, 1119 (1962) [Trans.: Bull. Acad. Sci. USSR, Phys. Ser. 26, 1127 (1962)].
- 11) E. Amaldi and F. Rasetti, Ricerca Sci. 10, 115 (1939).
- 12) H. Rauch, F. Grass and B. Feigl, Nuclear Instrum. Methods 46, 153 (1967).
- 13) B. Feigl and H. Rauch, Nuclear Instrum. Methods 61, 349 (1968).
- 14) A.P. Jeavons and C. Cate, IEEE Trans. Nucl. Sci. NS-23, 640 (1976).
- 15) G. Charpak, Annu. Rev. Nuclear Sci. 20, 195 (1970).
- 16) C. Parkman, Z. Hajduk, A.P. Jeavons, N. Ford and B. Lindberg, Proc. 2nd Ispra Nuclear Electronics Symposium (EURATOM, Luxembourg, 1975), EUR 5370e, 139 (1975).
- 17) A.P. Jeavons, N. Ford, B. Lindberg, C. Parkman and Z. Hajduk, IEEE Trans. Nuclear Sci. NS-23, 259 (1976).
- 18) G. Charpak, A.P. Jeavons, F. Sauli and R.J. Stubbs, CERN 73-11 (1973).